Pathol. Oncol. Res. (2009) 15:567–577
DOI 10.1007/s12253-009-9156-y

ORIGINAL PAPER

Aminobisphosphonate Stimulates Bone Regeneration and Enforces Consolidation of Titanium Implant into a New Rat Caudal Vertebrae Model

József Blazsek · Csaba Dobó Nagy · István Blazsek · Rita Varga · Bálint Vecsei · Pál Fejérdy · Gábor Varga

Received: 29 January 2009 / Accepted: 13 February 2009 / Published online: 7 March 2009

Abstract Bisphosphonates are widely used as therapeutic agents in bone disorders including cancer metastasis due to their osteoclast inhibitory effect. Recent data shows that bisphosphonates may also induce bone-building by stimulating osteoblast activity. Clinical observations, however, have revealed that bisphosphonates may cause necrosis in the oral cavity which questions their usefulness in bone regeneration during the consolidation of inorganic implants. Here we report the investigation of bone neogenesis following chronic amine bisphosphonate (Zometa®) treatment in a novel experimental model, using the rat tail vertebra as a support. This method involves (1) implantation of titan screw into the tail vertebrae, (2) systemic bisphosphonate treatment and (3) quantitative biophysical measurements which mirrors consolidation of implant, i.e. strength of fixation and changes in newly formed bone architecture using micro Computer Tomograph (micro-CT). The degree of fixation of titan implants (osseointegration) increased by 36% on the effect of Zometa and the structure of newly formed bone became robust. The mass of new bone increased 3.1-fold at 6 weeks of regeneration, as compared to controls. Thus, Zometa®, a potent aminobisphosphonate used in therapy of cancer metastases, osteoporosis and bone marrow transplantation, significantly increased bone neogenesis and enforced osseointegration of titan implants as measured quantitatively in the rat tail vertebra. Our data support the usefulness of aminobisphosphonates in the rehabilitation of bone loss as well as in improvement osseointegration of implants. We emphasise that this novel method may open up new possibilities for screening the effects of local and systemic treatments.

Keywords New implant osseointegration model · Osteo-neogenesis · Aminobisphosphonates (Zometa®) · Bone regeneration · Micro computer tomography (micro-CT) · Biomechanical measurement

J. Blazsek (✉)
Department of Oral Biology, Semmelweis University,
Nagyvárad tér 4.,
Budapest 1089, Hungary
e-mail: blajozs@net.sote.hu

C. Dobó Nagy · B. Vecsei · P. Fejérdy
Department of Prosthodontics, Semmelweis University,
Budapest, Hungary

I. Blazsek
INSERM U602 and U972, ICIG and Université de Paris-Sud,
Paul-Brousse Hospital,
94807 Villejuif, France

R. Varga
Full-Tech Company,
Budapest, Hungary

G. Varga
Department of Oral Biology, Semmelweis University,
Budapest, Hungary

Introduction

The integrity and strength of vertebrate skeleton is maintained by continuous formation and resorption of the crystallized bone tissue via osteoblasts and osteoclasts, respectively [1, 2]. Under homeostasis the bone steady state is modulated by mechanical usage, by central and local endocrine control and by short-range "cross-talk" between cells in the bone/bone marrow microenvironment [3, 4]. Recently, it has also been appreciated that a close association exists between bone and vasculature at specific micro-domains, called "bone remodelling compartment" (BRC) [5, 6], that plays a pivotal role in bone remodelling

and fracture repair. The BRC is surrounded by flattened bone lining cells. Osteotropic growth factors and cytokines (osteoprotegerin, RANKL) have been identified in bone lining cells inside a confined space separated from the bone marrow which allows local regulation. Acquired bone diseases thus may result from perturbations to bone marrow derived osteoblasts, to hematopoietic stem cell derived osteoclasts, to vascular endothelium or from loss of balance between the BRC compartment and surrounding bone lining cells [7, 8]. BRC creates a domain where cells directly interact with denuded bone and bone matrix, and it can be hypothesized that it represents a preferential base plate ("window") for seeding of bone specific metastatic cells. Metastatic cells, mainly breast and prostate cancer cells and multiple myeloma cells are endowed with the capacity to promote the formation and function of osteoclasts by producing parathyroid hormone-related protein (PTHrP) [9]. Consequently, reduction of the BRC area by anti-resorptive therapy, such as bisphosphonates, could significantly reduce the incidence of skeletal metastatic event [1, 6, 10, 11].

Despite its robustness, the bone tissue is highly susceptible to pathophysiological perturbations due to aging, endocrine unbalance, microbial infections and inflammatory reactions, irradiation or other therapy-related side effects and also cancer. All these perturbations progress towards mechanical trauma the cure of which represents a severe problem in human health care. Important progress has been achieved recently in the surgical treatment of bone diseases. The recent burden in searching for new scaffold materials, osteotropic factors, combined with gene therapy [13] and local stem cell delivery [14, 15], all have opened up new avenues to develop optimal treatment schedules for bone repair.

A major methodological problem, which still needs further improvements, concerns the use of metal implants especially in dental rehabilitation. The difficulty to obtain long-lasting consolidation arises from the nature of interface phenomenon (ingrowth into porous surface, adherence) which is different from the phenomenon of cell-to-cell adhesion [16–18]. In other fields of tissue engineering the use of biological glues to reinforce surface adherence, for example chondroitin sulphate for cartilage tissue-biomaterial integration, has resulted in strong consolidation [19]. In the case of bone-metal interaction the basic cellular interplay between osteoblasts and osteoclasts, that maintain tissue homeostasis, should be directed toward building of less porous bone tissue. Bisphosphonates is used for the treatment of osteoporosis, due to their inhibitory effects on osteoclast genesis and activity [10, 20–23]. Their side effects, however, represent an important limitation mostly in elderly patients [24–26]. Zometa, a heterocyclic imidazol bisphosphonate, appears to be less toxic at lower, active dose regimens, when compared to more established bisphosphonates. In addition, recent data revealed, that it may enhance the proliferation and stimulate terminal differentiation of preosteoblastic cell lines in culture [27–29]. Furthermore short-term Zometa treatment increases bone mineral density and the number of marrow clonogenic fibroblast progenitors after allogeneic stem cell transplantation [30].

These data have raised the question as to the effects of chronic Zometa treatment on osseointegration and bone structure. In order to investigate this question we have developed a novel in vivo experimental implantation model which allows the effect of systemic and/or local treatments to compare. This includes (1) implantation of titan screw of porous surface [31] into the rat caudal vertebrae, (2) systemic treatment schedules and, as an endpoint, (3) quantitative biomechanical measure which mirrors consolidation of the implant i.e. strength of fixation (*Newton* = *N*) and changes in architecture between steady state and newly formed bone using micro-CT. The method involves two novel approaches: the use of spongy tail vertebra as support and the creation of a thinner hole for the tip of implant which is surrounded by a shorter and larger "empty" cylinder around the implant. This method allows the local application of bio-materials and/or selected cell populations to be tested and to measure the effect on neo-ossification, while the screw holding a tiny ring at the proximal end, allows measurement of the implants' biomechanical properties, i.e.. the force of consolidation. The results we show here demonstrate the feasibility of operation and document that Zometa® in chronic systemic treatment increased the newly formed bone mass around the titan implant.

Materials and Methods

Animals Female Wistar rats (Crl(Wi)Br, Charles River; 250–370 g) from the breeding colony of Semmelweis University were kept in light controlled, air-conditioned rooms and fed *ad libitum*. Rats were anesthetized with sodium pentobarbital (Nembutal 40 mg/kg body weight (b.w.), by intraperitoneal (i.p.) injection. C57BL/6 wild-type mice (IFFA CREDO, L'Arbresle, France) were bred under a 12-hour light-darkness schedule. For comparative anatomical and histological studies; mice were anesthetized by avertine, exsanguinated by intracardiac perfusion with 100 mL Ca, Mg-free PBS/20IU heparin/mL prior to fixation. (Ethical license of animal experiment N°: 46/1999 and 1799/003/2004)

Surgical Placement of Titanium Implants The tail was disinfected and ligatured to control bleeding during surgery. A 5–6 mm incision was made at the level of caudal C4–C5 vertebrae. The skin was retracted and the vertebrae were exposed under sterile conditions. In the exposed surface of C4, first, a central 1 mm diameter and 5 mm deep hole was

formed, which corresponds to the size of titanium screw, using an electric drill. Subsequently, a larger and shorter hole was made (2.0 mm diameter and 3.5 mm depth, Fig. 2.), thus creating an "empty" cylinder which allowed the prospective bone regeneration to be monitored. Screw-type titanium implants (1.2 mm in diameter; see Fig. 2b) were fabricated and their surface roughened using sand-blasting (Full-Tech Company, Hungary). Sterilized screws were introduced into the 5 mm deep thin hole. Following insertion of the implant the skin was repositioned over the implant and tightly sutured. The surgical wound was protected aseptically by a plastic film-layer (Plastubol®: methylmethacrylat-butylacrylat-butylmethacrylat, diisooctyl phtalate—Pannonpharma Ltd.Hungary). Rats were kept in individual cages to insure appropriate hygiene and wound healing during the first two weeks following surgery.

Aminobisphosphonate (Zometa®) Treatment The cyclic amine-bisphosphonates Zoledronate (Zometa® Novartis) has been used according to the manufacturer's recommendation, applying 60% of the single lethal dose (1 mg/kg b.w.) established for rats. 0.6 mg/kg Zometa® was injected i.p. in 1 mL physiological saline; controls received 1 mL of physiological saline. Ten rats were included in both control and Zometa treated groups. The subsequent Zometa® treatments were done at 14 days intervals (on days 0, 14 and 28).

Determination of the Biomechanical Property, Fixation of the Implants and the Maximum Extraction Force Six weeks following the surgery rats were exsanguinated under Nembutal anaesthesia. Before removing the implants, the bony structure of all animals (n=10) from each group was scanned using the micro-CT. Following removal of the implants, vertebrae were fixed in 10% formalin and every surgically-treated vertebrae and references (two vertebrae of each animal), were scanned using the micro-CT. The maximum force needed to extract the titanium implant was measured using a Tenzi TE 18.1 (TENZI Ltd. Hungary) apparatus and expressed in Newton (N). Measurements were done as follows: a) the proximal end of implant was opened and a thin steel wire was thread through to provide an appropriate grip for the measuring device; b) after the vertebra was fixed and the instrument was normalized, the implant was steadily pulled along its long axis until completely extracted; c) the maximum reading on the instrument during displacement was recorded as the maximum force (N) needed to counter osseointegration.

Micro Computer Tomography (micro-CT) a) 6 weeks following the placement of titanium implants bone regeneration was measured using an X-ray micro-CT instrument (SKYSCAN 1172 X-ray Microtomograph, Belgium). The instrument had an X-ray source from a sealed microfocus X-ray tube with a spot size of 8 µm, a resolution of 17.7 µm, and uses a cone-beam volumetric reconstruction algorithm. We used a 0.5 mm aluminium filter to "soften" and even-out the X-ray beams. b) Implanted samples were scanned at 360° rotation while the bony socket of the vertebra following removal of the implants were scanned with 180°, at 0.7 degree intervals. The X-ray scatter generated on the surface of the implants was subtracted. c) For reconstruction of 2D and 3D images we used the cone-beam volumetric algorithm (Feldkamp). d) Measurements were made on the Region of Interest (ROI) × 1.5 mm Tissue Volume (TV) on the computer-reconstructed 3D samples. These measurements were made both before and after removal of the implants.

Reconstruction and 2D Analysis 2D and 3D images were reconstructed and data were analyzed using the Skyscan software. First, we determined the original dimensions of the "empty" bony chamber that were originally created using burs. We also determined the volume of the inserted implant. Finally, we subtracted the two volumes to determine the volume of the newly generated bone tissue. This "Tissue Volume" (TV) was the area between the implant surface and the walls of the bony chamber. TV had a thickness of 1.5 mm and a total of 86 scanned consecutive layers (ROI× 1.5 mm TV=2.694 mm^3) were analyzed using the Skyscan software. To provide an additional internal control, we also scanned the vertebrae immediately above the one that was treated with implant (Fig. 5: a,b and c,d). In these vertebrae the tested tissue volume was identical (TV=2.694 mm^3) to the prepared vertebrae. Thus we have four data groups: A - Reference Bone Control; B - Reference Bone—Zometa® treated; C - New Bone—control; and D - New Bone—Zometa® treated. The results of analyses for these four groups are shown in Table 1. Data were compared for significance using standard statistical software.

Whole Mount Staining of Bone and Cartilage The skeleton was cleaned, fixed and dehydrated in 50, 70 and 100% ethanol and three changes in acetone. Alizarin red/alcian blue staining was carried out in standard staining solution (5 vol. 0.3% alcian blue in 70% ethanol, 5 vol. 0.1% alizarin red in 96% ethanol, 5 vol. acetic acid and 85 vol. 70% ethanol) overnight at 37°C. Background coloration was removed by several changes in 1% KOH, 20% glycerine in water [32, 33]. Native or stained skeleton preparations were photographed using dark-field illumination under a Zeiss STEMI SV8 stereomicroscope attached to a SONY CCD camera. Representative fields were mounted using Photoshop.

Histology Vertebrae and femur were dissected, cleaned and fixed overnight in acetic acid-zinc-formalin (AZF) fixative (1.25 g zinc chloride, 15 mL cc formaldehyde, 0.75 mL

glacial acetic acid and distilled water (d.w.) to 100 mL) at room temperature . Following three washes in d.w. for 30 min Gooding and Stewar's decalcification fluid was added for 4 h (10% formic acid, 5% formaldehyde in water). Samples were washed in water before processing for sucrose-gelatine impregnation and freezing in isopenthane at −80°C. Sections, 5 to 10 μm thick, were cut in a freezing microtome, placed on poly-lysine coated slides and were processed for differential staining [32]. Osteoblasts were identified by strong alkaline phosphatase and osteoclasts by tartarate resistant acid phosphatase (TRAP) reactivity using standard detection kits (Sigma, USA). In other experiments the vertebrae were fixed in formaldehyde for 2 days, and were decalcinated in 18% sodium-EDTA (pH 7.4) solution for one week at 56°C and were embedded into paraffin. Dewaxed sections were stained routinely with hematoxylin and eosin, periodic acid-Schiff (PAS) reagent and silver nitrate. After mounting slides were photographed in Leica DMLB1005 light microscope equipped with a JVC LCD camera.

Statistical analyses Values represent mean ± standard deviation (S.D.). The data of stabilization force were performed using 10–10 parallel samples. A morphometric analysis was applied for both internal and external controls. Comparison among the groups was performed by ANOVA (Student's *t*-test). Calculations were performed using the InStat program package (GraphPad Software, Inc., San Diego, CA).

Results

Rational Use of Tail Vertebras for Implantation Studies

In preliminary experiments, searching for a massive, spongy bone compartment, amenable at supporting titanium implants, we observed that similarly to the sacral vertebrae, caudal (tail) vertebrae are also constituted by an abundant spongiosa delimited by the cartilage (Fig. 1a and 1b). However, stereomicroscopy of native preparations (Fig. 1c and 1d) and enzyme histology showed that the bone marrow parenchyma was much less in the tail vertebrae than in the hematopoietic femur. Osteoclasts are abundant as revealed by TRAP (Fig. 1e and 1f), suggesting that tail vertebrae may provide an ideal tissue support for implant studies, for the delivery of biomaterials and for the analysis of drugs interfering with osteoclasts and/or osteoblasts regulation, in process of bone remodeling.

General Effects of Zometa®

Experiments in rats (unpublished results, Blazsek J et al.) and clinical data from the literature on distraction osteogenesis [34] indicated that bone regeneration can be systematically evaluated following 6 to 12 weeks of intervention. Systemic Zometa® treatment does not affected b.w. of young adult rats. On average, a rat gained approximately 4 g b.w. per week. Compared to controls, Zometa® treatment yielded no significant differences in b.w. (on day0: control rats weighted 288.6±29.3 g and Zometa® treated rats 292.7±21.6 g, $p>0.72$ NS, and after 6 weeks: they weighted respectively 312.8±33.7 g and 307.2±24.0 g, $p>0.66$, NS). Intraperitoneal injections did not lead to infection or inflammatory reaction in either of the animals. Importantly, the animals did not show any signs of infection at the site of surgery, nor side effect (osteonecrosis) following Zometa® treatment (Fig. 2c).

Aminobisphosphonate treatment for 6 weeks, in the absence of titanium implant, did not change the general histological aspects of osteoid trabecule at the subepiphyseal region. However, it was noted that the density of those trabeculi increased in treated animals (Fig. 3a,b). The PAS positive areas (non-calcified new bone) in neo-trabeculi did not change in treated animals suggesting an accelerated formation of calcified trabeculi. This was confirmed when silver impregnation was used to specifically label calcified areas in neo-trabeculi, which demonstrated enlarged regions in treated animals (Fig. 3c,d).

Evaluation of Bone Regeneration and Stability of Implants

Tail vertebrae, titanium implant and surrounding empty area were prepared as detailed in Materials and Methods. The schematic representation of tail vertebra, drilling instruments and empty place created for bone neogenesis are shown on Fig. 2.

Figure 4 shows the force that was needed to remove the implants in control and Zometa® treated animals after 6 weeks of implantation. These values represent the degree of bone regeneration and stability of implants. These data are typical to those seen during normal bone regeneration. The average force needed to remove the implants from Zometa® treated animals was 44.2±14.4 N, compared to controls 32.4±9.4 N. Although the Zometa® treated group had a 35% higher value, statistical analysis revealed no significance ($p<0.06$).

Morphometric Evaluation of Bone Generation Using High Resolution Micro-CT Analysis

Micro morphometry and micro-CT morphometric measurements were done on a predefined area (TissueVolume (TV)= ROI×1,5 mm=2,694 mm^{33}) (Fig. 5), as indicated on Fig. 7a–d.

A reconstructed 3D image of the tail vertebra is shown on Fig. 6a, the longitudinal section on Fig. 6b and

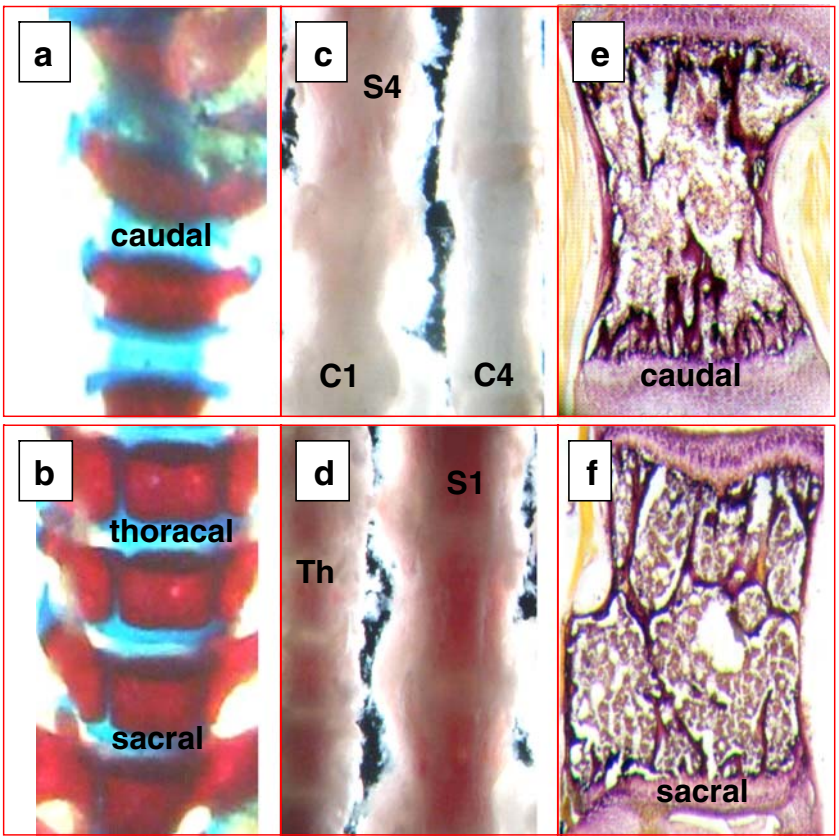

Fig. 1 Comparative histology of tail vertebrae and other spongy bone marrow compartments. The caudal (**a**) and thoracal-sacral (**b**) vertebrae have similar bone (Alizarin red) and cartilage (Alcian blue) constitution as revealed by double staining and tissue vitrification. Native preparations show a striking difference in red bone marrow parenchyma, which is quasi-absent in the tail vertebra (**c**) and abundant in the thoracal-sacral vertebrae (**d**). Low power magnification enzyme histology of tail (**e**) and femur (**f**) show the abundance of TRAP positive osteoclasts in tail vertebrae and the abundance of marrow parenchyma in femur

cross section following extraction of implant on Fig. 6c Computer Tomographic 3D images of ROI×1,5 mm are shown 6 weeks after control treatment (Fig. 6d). Note that Zometa® induced (Fig. 6e) a three-fold increase in new bone formation: (Fig. 7, $p<0.002$), increased both the thickness and doubled the number of trabecule (Fig. 8, $p<0.002$), and reduced the volume of inter trabecular space i.e. bone density three-fold (Table 1).

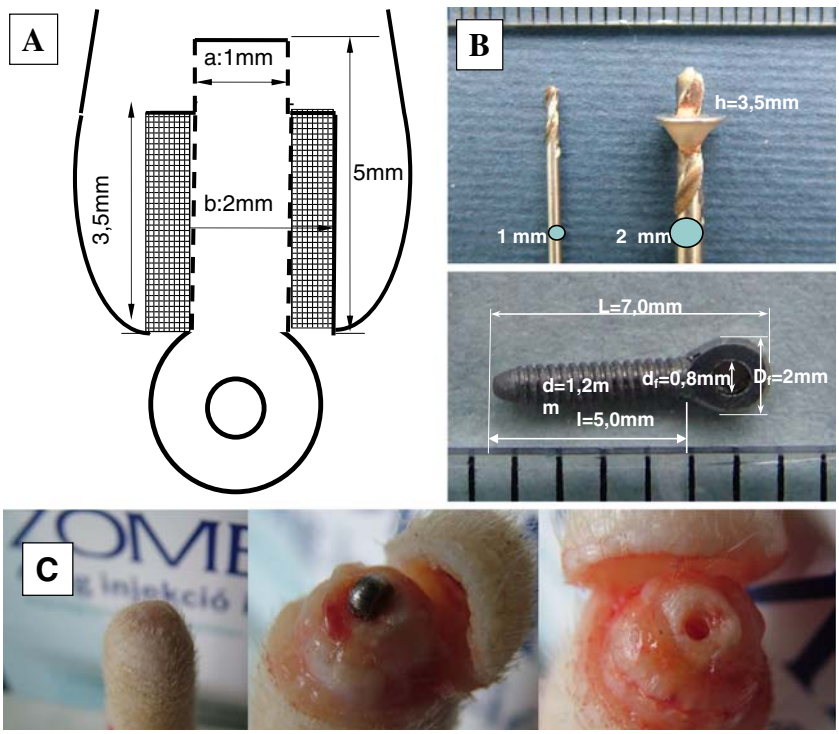

Fig. 2 **a** Schematic representation of tail vertebra containing preformed hole for the titanium implant (*dotted lines*) and the empty place created for bone neogenesis (*checked area*). **b** Drilling instruments (*upper*) for preparing the holes for the titanium implant (*under*) and for the empty, cylinder surrounding the implant permitting bone regeneration measurement. (*see* Materials and Methods). **c** Wound heeling at the distal tail vertebra (*left*) and bone regeneration before (*middle*) and after retraction of the implant (*right*). Note, that there was no inflammatory reaction around the implant following 6 weeks of Zometa treatment post-operation

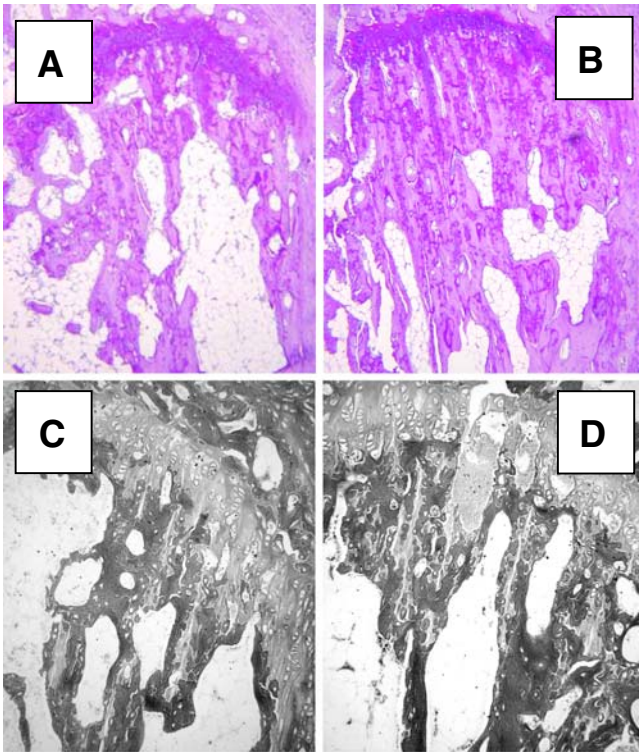

Fig. 3 Comparative histology at the subepiphyseal region in sham-implanted rat tail vertebra 6 weeks after operation: control (**a**, **c**) and Zometa treated (**b**, **d**) samples following PAS reaction (**a**, **b**) and silver impregnation (**c**, **d**). Note the irregular osteoid trabeculi with a moderate amount of PAS-positive material in control (**a**) and the increased amount of osteoid trabeculae with moderate amount of PAS positive materials (*pink color*) following Zometa treatment (**b**) (magn.100×). Silver impregnation indicates a moderate amount of calcified osteoid component in control vertebra (**c**), and the strongly calcified osteoid trabeculi following Zometa treatment (**d**) (magn. 200×)

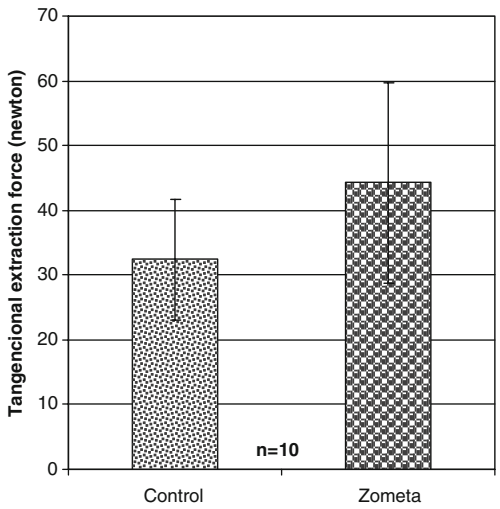

Fig. 4 The strength of titan implant osseointegration increased by 36% following Zometa treatment for 6 weeks (control: 32.4±9.38 Newton; Zometa: 44.22±15,38 Newton; $p<0.06$)

The results of quantitative morphometric analysis of bone generation are presented on Figs. 7, 8 and Table 1. On the control and Zometa® treated animals a constant volume (ROI×1.5 mm=2.694 mm^3-Tissue Volume (TV)) was scanned, both of the intact C3, surgically untreated "Reference" bone (marked "A" and "B") and at the subsequent (C4), surgically implanted "New" bone (marked "C" and "D").

The morphometric values for this control ("A" Reference Bone—Control) are shown in Table 1. The total amount of bone found in this scanned constant volume was 57.72%. The total volume of the bone in the above scanned volume was 1.55 mm^3 with a surface area of 38.75 mm^2. The number of trabecule was 7.192/mm, (5.353/mm rod model), the average diameter of the trabecule was 160.93 µm (rode model), and the average trabecular ½ thickness was 40.23 µm. The interlamellar space (trabecular separation = Tb. Sp.) is 59.08 µm (26.73 µm rod model).

In Zometa treated animals ("B") there were no significant changes, compared to controls. The total volume of the new bone was 50.78%, slightly less when compared to controls in column A (57.72%); its volume was 1.368 mm^3, its surface was 35.79 mm^2, the number of trabecule was 6.64/mm (5.31/mm—rod model), the diameter of the trabecule was 152.23 µm (rode model) and the average ½ thickness of the trabecule was 38.05 µm. There was no significant difference among the two sets of control data (Table 1: A and B, Figs. 7–8). But the interlamellar space (Tb.Sp.) was significantly ($p<0.03$) larger—75.00 µm (37.06 µm rod model)—in reference bone of Zometa® treated animals.

The third set of data represents those from the surgically treated but Zometa® untreated animals ("C" - New Bone—Control). We scanned the constant volume (TV) of 2.694 mm^3 of bone one and found that the 6-weeks old regenerated bone in this group represented only 21.67%, with a volume of 0.583 mm^3 and a surface area of 25.223 mm^2. The number of the generated bone trabecule was less (−34.9%) than controls 4.682/mm (5.77/mm rod model), with significantly smaller diameter for the trabecule 89.77 µm (rod model) and the lamellae were close to 50% thinner with a 22.445 µm ½ thickness. Between the lamellae there was more than three-fold larger space when compared to standard bone. In accord with these data, the interlamellar space (Tb.Sp.) 179.63 µm–84.95 µm rod model—was markedly larger here in the "new" bone controls (ABD–C ****$p<0.002$), than in the Zometa® treated group

Finally, from data presented in Table 1 (column "D"- New Bone—Zometa®) and Figs. 7 and 8 it is obvious that Zometa®—treatment stimulated bone regeneration. In the scanned 2.694 mm^3 constant (TV) area 63.8% of its volume represents new calcified bone. This has a volume of 1.72 mm^3, with a surface area of 35.4 mm^2, with a number of trabecule of 6.58/mm (4.661/mm—rod model), diameter of the trabecule of 195.5 µm (rod model)—its significant, two-

Table 1 Comparative micro-Computer tomograph analysis of rat tail vertebra in controls and Zometa treated rats after 6 weeks of treatment

Reference bone		**"B" Reference-bone ZOMETA**		**"A" Reference-bone control**		**B–A%**	**"AB" $p<$**
$n=10$,	unit	means	*Sd*	means	*Sd*	Δ %	significance
Tissue volume (TV) (= ROI×1,5 mm)	mm^3	2,69	*0*	2,69	*0*	0	NS
Percent bone volume (BV/TV)	%	**50,78**	*9,62*	**57,72**	*5,08*	−12,0	$5{,}8\times10^{-2}$
Tissue surface (TS)	mm^2	19,90	*0,42*	19,92	*0,43*	−0,1	NS
Bone surface / Bone volume ratio (BS/BV)	1/mm	26,80	*4,22*	25,10	*2,40*	+6,7	NS
Trabecular separation (plate model Tb.Sp)	µm	**75,00**	*18,44*	**59,08**	*8,84*	+26,9	$2{,}4\times10^{-2}$
Trabecular diameter (rod model Tb.Dm)	µm	**152,23**	*23,14*	**160,93**	*15,45*	−5,4	NS
Trabecular separation (rod model Tb.Sp)	µm	37,06	*12,65*	26,73	*6,64*	+38,6	$3{,}4\times10^{-2}$
Trabecular number (rod model Tb.N)	1/mm	5,31	*0,36*	5,35	*0,38*	−0,7	NS
New bone		**"D" New-bone ZOMETA**		**"C" New-bone control**		**D–C%**	**"CD" $p<$**
$n=10$,	unit	means	*Sd*	means	*Sd*	Δ %	significance
Tissue volume (TV) (= ROI×1,5 mm)	mm^3	2,69	*0*	2,69	*0*	0	NS
Percent bone volume (BV/TV)	%	**63,80**	*12,87*	**21,67**	*9,58*	+194,4	$1{,}4\times10^{-7}$
Tissue surface (TS)	mm^2	20,79	*1,26*	21,07	*0,53*	−1,3	NS
Bone surface / Bone volume ratio (BS/BV)	1/mm	20,99	*3,60*	46,39	*9,20*	−54,8	$1{,}95\times10^{-7}$
Trabecular separation (plate model Tb.Sp)	µm	**59,97**	*35,20*	**179,63**	*56,85*	−66,6	$2{,}3\times10^{-5}$
Trabecular diameter (rod model Tb.Dm)	µm	**195,50**	*32,21*	**89,77**	*20,31*	+117,8	$6{,}34\times10^{-8}$
Trabecular separation (rod model Tb.Sp)	µm	23,15	*23,38*	84,95	*21,79*	−72,7	$8{,}92\times10^{-6}$
Trabecular number (rod model Tb.N)	1/mm	4,66	*0,68*	5,77	*0,57*	−19,2	9×10^{-4}

Characteristic quantitative parameters were measured in the control and Zometa treated groups and in the original Reference Bone ("A" and "B") and 6 weeks after regeneration in the New Bone ("C" and "D")

times higher than "C" new bone control—and ½ thickness of lamellae of 48.88 µm ($p<6.34\times10^{-8}$). The Zometa®—treated animals demonstrated almost a three fold increase in new bone formation while the Standard Bone (surgically untreated vertebra) was not affected. The interlamellar space (Tb.Sp.) 59.97 µm–23.15 µm rod model—which is thinner, than untreated samples; namely this new regenerated bone is robustness as a consequence Zometa® medication.

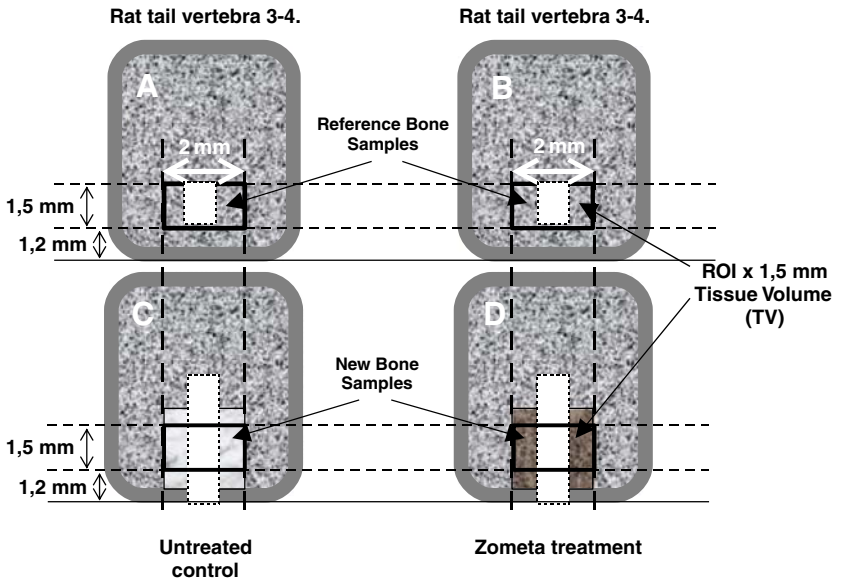

Fig. 5 Topological representation of micro-CT morphometric measurements on the Reference tail bone : **a** control untreated, **b** control Zometa treated group, **c** implant holding untreated control, **d** Zometa treated implant holding group. The analyzed tissue volumes (TV=2.694 mm^3) were allocated as Region-Of-Interest (ROI) corresponding to the cylindrical "free place" allowing bone regeneration at a 1.5 mm path length (*black squares*). White squares show the place of the titanium implant that was excluded from the measurement

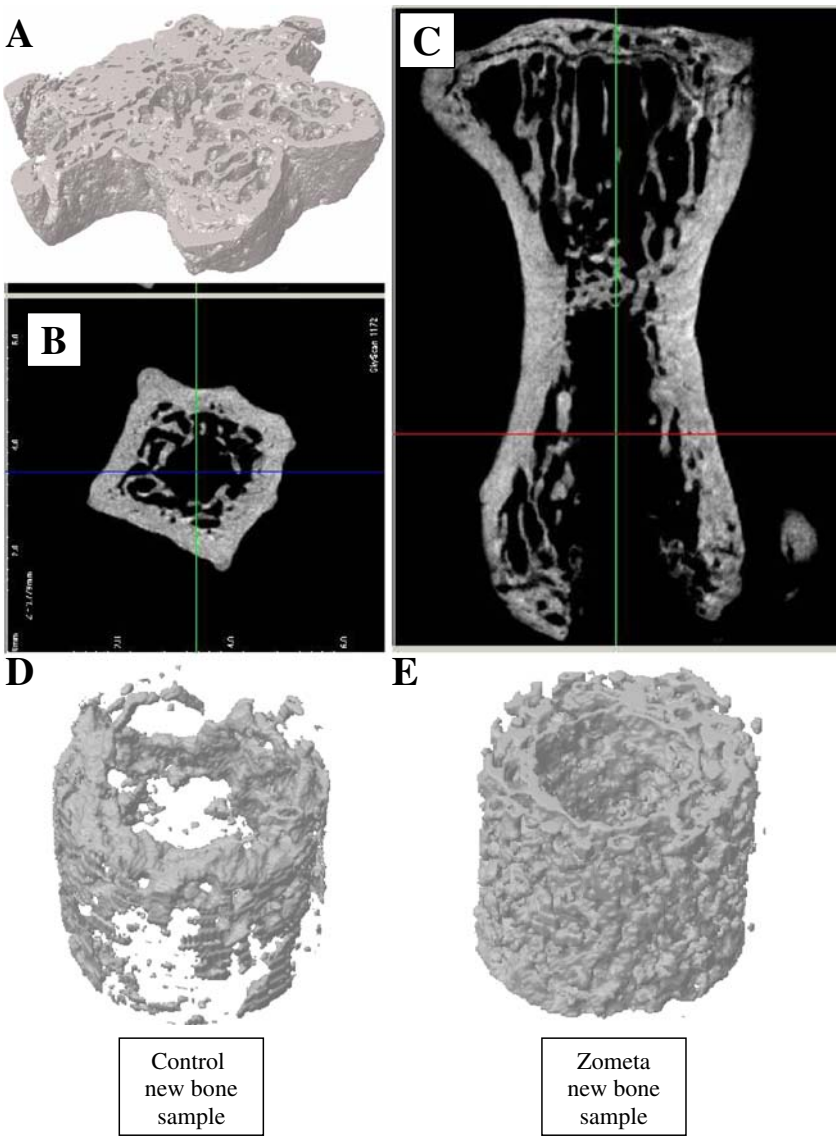

Fig. 6 micro-CT reconstruction images 6 weeks after treatment. **a** 3D image of the tail vertebra with implant from Zometa-treated group, **b** cross section and **c** longitudinal section before extraction of the titanium implant. Note the trabeculi of spongy bone, the surrounding compact bone and the implant. Fig. 6d) and Fig. 6e) are 3D image of ROI × 1,5 mm. Zometa treatment induced a three-fold increase in new bone formation: 6d) control = 0.58±0.26 mm^3 and 6e) Zometa 1.72±0,35 mm^3; ($p<0.002$), increased the thickness of trabecules twice ($p<0.002$), and reduced the volume of intra trabecular space (i.e. bone density) three-fold

Discussion

The force and longevity of integration of foreign materials into the bone tissue represent a major problem in tissue engineering. Because of the difficult accessibility of the mandibula and maxilla different research teams have succeeded in measuring osseointegration mainly in anatomically accessible bone compartments i.e. in haematopoietic femur [31]. In this work we developed a novel, versatile in vivo test system, amenable at quantifying bone neogenesis under different experimental conditions. The tail vertebrae appeared useful to create a tissue environment where the force of integration of titanium implants, due to bone neogenesis, can be evaluated by biomechanical measurement, and the structure of newly formed bone could be analysed by micro-CT or histology. Our preliminary studies uncovered that the spongy tail vertebra is poor in BM parenchyma, however contains an elevated frequency of osteoblasts (I. Blazsek et al., unpublished) and TRAP positive osteoclasts, indicating the usefulness of tail vertebrae in several research fields of tissue engineering. The "empty" cavity created around the implant allows the controlled, local application of different substitution materials: mesenchymal stem cells, growth and differentiation factors or biological glues [19] either alone or in combination with systemic medicament.

Having the optimized model in hand we addressed whether Zometa®, a novel amino bisphosphonates, used in cancer therapy to reduce bone metastasis of prostate and breast cancer cells, could accelerate bone regeneration. According to classical notions, the primary effect of bisphosphonates resides in moderation of bone resorbtion via inhibition of osteoclasts [10, 11]. Amine bisphosphonates act on the mevalonate cycle by inhibiting farnesylpyrophosphate syn-

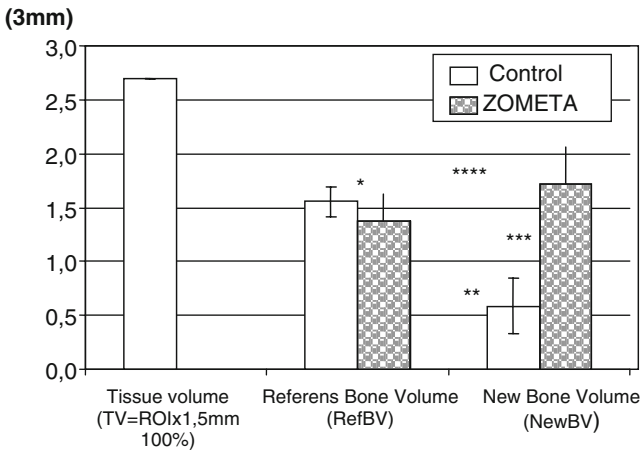

Fig. 7 Comparison of bone volume parameters. Zometa treatment significantly increases the volume and mass of newly formed bone tissue. The analyzed tissue volume—which is ROI×1.5 mm= 2.694 mm^3—(TV=100%), the reference bone volume (Ref-BV) and the volume of newly formed bone tissue (New-BV) are shown in controls and Zometa treated rats at 6 weeks of treatment. There was no significant difference in the Reference Bone tissues (NS); the volume of regenerating new bone was significantly less in the control group ($p<0.002$), while the new bone volume of Zometa treated group reaches the value of the Reference (NS $p>0.05$). The NewBV was more than three-fold higher in the Zometa group, compared to controls ($p<0.002$)

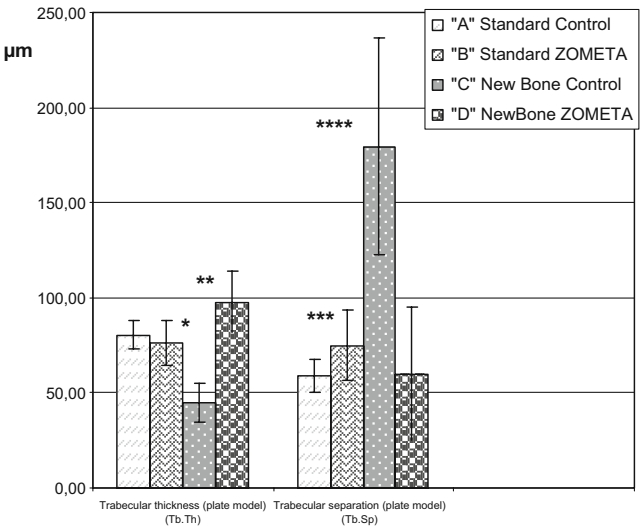

Fig. 8 The half trabecular thickness (µm; bone volume per surface), Bone surface (mm^2) and the number of trabecules (1/mm) were measured in controls and Zometa treated rats within the predefined normal reference area bone and newly formed bone area. Zometa had no effect on reference bone, however, the control regenerating bone was remarkably retarded as compared to the normal reference bone ($p<0.002$), and significant differences were measured between the non-treated and Zometa treated groups ($p<0.002$). The bone surface was reduced significantly in controls ($p<0.002$), systemic Zometa treatment increased bone formation: by 6 weeks bone surface reached the control reference value ($p<0.002$). The trabecular number is same in reference bone both of untreated and Zometa treated group(NS), but was retarded significantly in new bone of untreated rats ($p<0.002$). The number of trabeculae in new bone is significantly higher (40.6%) in the Zometa treated group than untreated group and it was same the trabeculae number of reference bone

thase [21], which is indispensable for the prenylation of GTP-binding proteins (Rab, Ras, Rho, Cdc42). A decrease in these regulatory proteins results in inhibition of osteoclast function [20, 22]. The hypothesis, that bisphosphonates may act on bone formation directly, by stimulating osteoblast functions, has also been experimentally demonstrated in vitro [28, 29]. Recently, it has been shown that treatment of patients with aminobisphosphonate following allogenous BM transplantation increased the frequency of colony forming mesenchymal preosteoblasts in BM [35]. These results, together, support the direct effect of bisphosphonates on bone-building osteoblasts and thus further reveals their potential dual effects.

In our experiments the bone volume increased threefold following Zometa® treatment as compared to control untreated rats. Taking the native, non-manipulated, non-treated bone volume as 100%, the bone volume of non-treated but implant holding rats was 37.5%, while the bone volume has reached 110.5% in the implant holding plus Zometa® treated group. There was negligible difference between the Zometa and reference groups, however the effect upon the number of trabeculae was significant causing 20% increase upon treatment with Zometa when compared to the new bone control group . Consequently, the structure of newly formed bone is composed by thinner trabecule and lamellae spaced by large alveoli in the control group, while in the Zometa® treated group the bone trabecule become thick and robust, 6 weeks after treatment. The physically measurable strength of consolidation of the implants has increased by 31 to 40%.

Thus, our results support that Zometa®, under disease-free regenerative conditions, stimulates bone formation. Remarkably, the highest positive effect was obtained when Zometa® and the titanium implant were associated. Indeed, titanium implant in the rat femur model induced expression of matrix metalloproteases (MMP-2, MMP-7, MMP-9), the tissue inhibitor of MP-3, TNF-alpha in osteocytes, osteoclasts. Also in hypertrophized chondrocytes and in vascular components [35] application of bisphosphonates, that preferentially fix to osteoclasts [36] where shown to inhibit both osteoclastogenesis, resorptive functions and may also induce apoptosis [2, 21, 37].

In addition to their use in oral pathologies, bisphosphonates have been successfully applied for the treatment of osteoporosis [10, 21–23], breast and prostate cancer metastases [6, 9–12], hypertrophic pulmonary osteoarthropathy [38] and fibrous dysplasia [39]. Recent recognition that application of bisphosphonates may be associated with side effects, mainly osteonecrosis of the jaw (ONJ) represents a mild limitation. Provided by a large-scale

evaluation: the risk of ONJ in case of osteoporosis is estimated between 1 in 10,000 and <1 in 100,000 patient-treatment years. However, in cancer patients treated with high doses of intravenous bisphosphonates the risk of ONJ is significantly higher (1–10 per 100 patients) [26]. It can be hypothesized that deleterious side effects which may occur in the oral cavity during bisphosphonate therapy cannot be attributed exclusively to bisphosphonates, rather to the complex and multifactorial background of diseased patients, resulting in different and very changeable oral microflora. Indeed, an emerging notion indicates that the timing and single dosage schedules, influences the therapeutic efficacy and side effects due to the direct action of bisphosphonates on osteoclasts [40, 41]. Taking available information from the literature and our results together, the data supports that bisphosphonates possess dual effects, acting both on bone building osteoblasts [28–30] and on bone resorbtion by osteoclasts [10, 36, 42].

In conclusion, 1) the results demonstrate that bone regeneration and osseointegration can be measured using the novel rat tail vertebra model. The experimental protocol that we described here for the first time may be useful in other situations where the quantitative and qualitative evaluation of new bone formation, in response to systemic or local treatments, is of primary importance. 2) Using this method we could quantitatively evaluate the stimulatory effect of Zometa® on bone neogenesis. 3) Another surprising outcome of this work was the recognition that spongy tail vertebras are poor in bone marrow parenchyma, but rich in bone forming and resorbing cells. This recognition has importance in several fundamental aspects. First, it support that the tail vertebrae is an ideal microenvironment for large-scale preclinical screening of bone modifying substances, with minimal interference upon bone marrow cells, a situation which also characterizes the jaw compartment. 4) The paucity of BM parenchyma in tail vertebrae provides an experimental tool in which the regulatory interaction between hematopoietic stem cells and their putative osteoblastic niches can be investigated [5, 43, 44]. Finally, previous publications [45] and our ongoing experiments on this field suggest that deciphering the pseudo-aplastic situation in tail vertebrae may also shed light on the cellular dysregulation which underlies the initiation and/or progression of myelodysplasic and preleukemic syndromes [46] in the hematopoietic bone marrow.

Acknowledgments The authors wish to thank Miklós Kovács and Márta Fülöp for skilled technical work, Tivadar Zelles and György Simon for critical discussions (USN), Ferenc Fullér (Full-Tech) for providing titanium implants and Claude Boucheix (InsermU602) for their continuous help. The authors wish to thank Neil Dixon (Manchester, UK) for critical reading of the manuscript. This work was supported in part by the Hungarian National Scientific Research Fund (OTKA61543 and IN67250), by the Hungarian Health Research Council (ETT332/2006) and by Inserm U602, ICIG and Université de Paris-Sud Kremlin-Bicètre, France.

References

1. Ducy P, Schinke T, Karsenty G (2000) The osteoblast: a sophisticated fibroblast under central surveillance. Science 289:1501–1504
2. Teitelbaum SL (2000) Bone resorption by osteoclasts. Science 289:1504–1508
3. Skillington J, Choy L, Derynck R (2002) Bone morphogenetic protein and retinoic acid signalling cooperate to induce osteoblast differentiation of preadipocytes. J Cell Biol 159:135–146
4. Ichida F, Nishimura R, Hata K, Matsubara T, Ikeda F, Hisada K, Yatani H, Cao X, Komori T, Yamaguchi A, Yoneda T (2004) Reciprocal roles of Msx2 in regulation of osteoblast and adipocyte differentiation. J Biol Chem 279:34015–34022
5. Hauge EM, Ovesel D, Eriksen EF, Mosekilde L, Melsen F (2001) Cancellous bone remodelling occurs in specialized compartments lined by cells expressing osteoblastic markers. J Bone Miner Res 16:1575–1582
6. Eriksen EF, Eghbali-Fatourechi GZ, Khosla S (2007) Remodeling and vascular spaces in bone. J Bone Miner Res 22:1–6
7. Kim JB, Leucht P, Luppen CA, Park YJ, Beggs HE, Damsky CH, Helms JA (2007) Reconciling the roles of FAK in osteoblast differentiation, osteoclast remodeling, and bone regeneration. Bone 41:39–51
8. Zaidi M (2007) Skeletal remodeling in health and disease. Nature Med 13:791–798
9. Guise TA, Yin JJ, Taylor SD, Kumagai Y, Dallas M, Boyce BF, Yoneda T, Mundy GR (1996) Evidence for a causal role of parathyroid hormone-related protein in the pathogenesis of human breast cancer-mediated osteolysis. J Clin Invest 98:1544–1549
10. Rodan GA, Martin TJ (2000) Therapeutic approaches to bone diseases. Science 289:1508–1514
11. Michaelson MD, Smith MR (2005) Bisphosphonates for treatment and prevention of bone metastases. J Clin Oncol 23:8219–8223
12. Boissier S, Ferreras M, Peyruchaud O (2000) Bisphosphonates inhibit breast and prostate carcinoma cell invasion, an early event in the formation of bone metastases. Cancer Res 60:2949–2954
13. Zhao Z, Wang Z, Ge C, Krebsbach P, Franceschi RT (2007) Healing cranial defects with AdRunx2-transduced marrow stromal cells. J Dent Res 86:1207–1211
14. Laino G, d'Aquino R, Graziano A, Lanza V, Carinci F, Naro F, Pirozzi G, Papaccio G (2005) A new population of human adult dental pulp stem cells: a useful source of living autologous fibrous bone tissue (LAB). J Bone Miner Res 20:1394–1402
15. Ohazama A, Modino SA, Miletich I, Sharpe PT (2004) Stem-cell-based tissue engineering of murine teeth. J Dent Res 83:518–522
16. Bränemark PI, Zarb GA, Albrektsson T (1985) Tissue-integrated prostheses In: Osseointegration in Clinical Dentistry. Quintessence, Chicago, pp 211–232
17. Lundborg G, Besjakov J, Bränemark PI (2007) Osseointegrated wrist-joint prosthesis: a 15-year follow-up with focus on bony fixation. Scand J Plast Reconstr Surg Hand Surg 41:130–137
18. Evans EA, Calderwood DA (2007) Forces and bond dynamics in cell adhesion. Science 316:1148–1153
19. Wang DA, Varghese S, Sharma B, Strehin I, Fermanian S, Gorham J, Fairbrother H, Cascio B, Elisseeff JH (2007) Multifunctional chonroitin sulphate for cartilage tissue-biomaterial integration. Nature Materials 6:385–392
20. Luckman SP, Hughes DE, Coxon FP, Russell RGG, Rogers MJ (1998) Nitrogen-containing bisphosphonates inhibit the mevalonate

pathway and prevent post-translational prenylation of GTP-binding proteins, including Ras. J Bone Mineral Res 13:581–589
21. Fisher JE, Rogers MJ, Halasy JM, Luckman SP, Hughes DE, Masarachia PJ, Wesolowski G, Reszka AA (1999) Alendronate mechanism of action: Geranylgeraniol, an intermediate in the mevalonate pathway, prevents inhibition of osteoclast formation, bone resorption, and kinase activation in vitro. Proc Nat Acad Sci USA 96:133–138
22. Van Beek E, Lowik C, Van Der Pluijm G, Papapoulos S (1999) The role of geranylgeranylation in bone resorption and its suppression by bisphosphonates in fetal bone explants in vitro: a clue to the mechanism of action of nitrogen-containing bisphosphonates. J Bone Mineral Res 14:722–729
23. Lee YP, Schwarz EM, Davies M (2002) Use of zoledronate to treat osteoblastic versus osteolytic lesions in a severe-combined-immunodeficient mouse model. Cancer Res 62:5564–5570
24. Merigo E, Manfredi M, Meleti M, Corradi D, Vescovi P (2005) Jaw bone necrosis without previous dental extractions associated with the use of bisphosphonates (pamidronate and zoledronate). J Oral Pathol 34:613–614
25. Farrugia MC, Summerlin DJ, Krowiak E, Huntley T, Freeman S, Borrowdale R, Tomich C (2006) Osteonecrosis of the mandible or maxilla associated with the use of new generation bisphosphonates. Laryngoscope 116:115–120
26. Khosla S, Burr D, Cauley J, Dempster DW, Ebeling PR, Felsenberg D, Gagel RF, Gilsanz V, Guise T, Koka S, McCauley LK, McGowan J, McKee MD, Mohla S, Pendrys DG, Raisz LG, Ruggiero SL, Shafer DM, Shum L, Silverman SL, Van Poznak CH, Watts N, Woo SB, Shane E (2007) Bisphosphonate-associated osteonecrosis of the jaw: report of a task force of the American Society for Bone and Mineral Research. J Bone Miner Res 22:1479–1491
27. Reinholz GG, Getz B, Pederson L, Sanders ES, Subramaniam M, Ingle JN, Spelsberg TC (2000) Bisphosphonates directly regulate cell proliferation, differentiation, and gene expression in human osteoblasts. Cancer Res 60:6001–6007
28. Fromigué O, Body JJ (2002) Bisphosphonates influence the proliferation and maturation of normal human osteoblasts. J Endocrinol Invest 25:539–546
29. von Knoch F, Jaquiery C, Kowalsky M, Schaeren S, Alabre C, Martin I, Rubash HE, Shanbhag AS (2005) Effects of bisphosphonates on proliferation and osteoblast differentiation of human bone marrow stromal cells. Biomaterials 34:6941–6949
30. Tauchmanovà L, Ricci P, Serio B, Lombardi G, Colao A, Rotoli B, Selleri C (2005) Short-term Zoledronic acid treatment increases bone mineral density and marrow clonogenic fibroblast progenitors after allogeneic stem cell transplantation. J Clin Endocrinol Metab 90:627–634
31. Ysander M, Branemark R, Olmarker K, Myers RR (2001) Intramedullary osseointegration: development of a rodent model and study of histology and neuropeptide changes around titanium implants. J Rehabilit Res Dev 38:183–190
32. Naresh KN, Lampert I, Haserjian R, Lykiis D, Elerfiel K, Horncastle D, Smith N, Murray-Brown W, Stamp GW (2006) Optimal processing of bone marrow trephine biopsy: the Hammersmith protocol. J Clin Pathol 59:903–911
33. Kaufman MH (1992) The atlas of mouse development. Academic, Harcourt Brace & Company, London
34. Saulacic N, Iizuka T, Martin MS, Garcia AG (2008) Alveolar distraction osteogenesis: a systematic review. Int J Oral Maxillofac Surg 37:1–7
35. Shubayev VI, Bränemark R, Steinauer J, Myers RR (2004) Titanium implants induce expression of matrix metalloproteases in bone during osseointegration. J Rehab Res Dev 41:757–766
36. Sato M, Grasser W, Endo N, Akins R, Simmons H, Thompson DD, Golub E, Rodan GA (1991) Bisphosphonate action. Alendronate localization in rat bone and effects on osteoclast ultrastructure. J Clin Invest 88:2095–2105
37. Coxon FP, Helfrich MH, Van't Hof R (2000) Protein geranylgeranylation is required for osteoclast formation, function, and survival: Inhibition by bisphosphonates and GGTI-298. J Bone Miner Res 15:1467–1476
38. Amital H, Applbaum YH, Vasiliev L, Rubinow A (2004) Hypertrophic pulmonary osteoarthropathy: control of pain and symptoms with pamidronate. Clin Rheumatol 23:330–332
39. Chapurlat RD, Hugueny P, Delmas PD, Meunier PJ (2004) Treatment of fibrous dysplasia of bone with intravenous pamidronate: long-term effectiveness and evaluation of predictors of response to treatment. Bone 35:235–242
40. Amant N, McDonald M, Godfrey C, Bilston L, Little D (2007) Optimal timing of a single dose of zoledronic acid to increase strength in rat fracture repair. J Bone Miner Res 22:867–876
41. Hashimoto T, Shigetomi M, Ohno T, Matsunaga T, Muramatsu K, Tanaka H, Sugiyama T, Taguchi T (2007) Sequential treatment with intermittent low-dose human parathyroid hormone (1–34) and bisphosphonate enhances large-size skeletal reconstruction by vascularized bone transplantation. Calcif Tissue Int 81(3):232–239
42. Mundy GR, Yoneda T, Hiraga T (2001) Preclinical studies with zoledronic acid and other bisphosphonates: Impact on the bone microenvironment. Semin Oncol 28(6):35–44
43. Blazsek I, Chagraoui J, Péault B (2000) Ontogenic emergence of the hematon, a morphogenic stromal unit that supports multipotential hemopoietic progenitors in mouse bone marrow. Blood 96:3763–3771
44. Calvi LM, Adams GB, Weibrecht KW, Weber JM, Olson DP, Knight MC, Martin RP, Schipani E, Divieti P, Bringhurst FR, Milner LA, Kronenberg HM, Scadden D (2003) Osteoblastic cells regulate the haematopoietic stem cell niche. Nature 425:841–846
45. Blazsek I, Goldschmidt E, Machover D, Misset JL, Benavides M, Comisso M, Ceresi E, Canon C, Labat ML, Mathe G (1986) Excess of lympho-reticular cell complexes in the bone marrow linked to T cell mediated dysmyelopoiesis. Biomed Pharmacother 40:28–32
46. Epling-Burnette PK, Painter JS, Rollison DE, Ku E, Vendron D, Widen R, Boulware D, Zou JX, Bai F, List AF (2007) Prevalence and clinical association of clonal T-cell expansion in Myelodysplastic Syndrome. Leukemia 21:659–667